Cancer Res Treat. 2005;37(2):114-121

Usefulness of Additional Delayed Regional F-18 Fluorodeoxyglucose Positron Emission Tomography in the Lymph Node Staging of Non-Small Cell Lung Cancer Patients

Young So, M.D., **June-Key Chung,** M.D., **Jae Min Jeong,** Ph.D., **Dong Soo Lee,** M.D. and **Myung Chul Lee,** M.D.

Departments of Nuclear Medicine and Thoracic Surgery, Seoul National University College of Medicine, Seoul, Korea.

Purpose: **In this study, we examined whether additional, delayed regional FDG PET scans could increase the accuracy of the lymph node staging of NSCLC patients.**

Materials and Methods: **Among 87 patients who underwent open thoracotomy or mediastinoscopic biopsy under the suspicion of NSCLC, 35 (32 NSCLC and 3 infectious diseases) who had visible lymph nodes on both preoperative whole body scan and regional FDG PET scan were included. The following 3 calculations were made for each biopsy-proven, visible lymph node: maximum SUV of whole body scan (WB SUV), maximum SUV of delayed chest regional scan (Reg SUV), and the percent change of SUV between WB and regional scans (% SUV Change). ROC curve analyses were performed for WB SUVs, Reg SUVs and % SUV Changes.**

Results: **Seventy lymph nodes (29 benign, 41 malignant) were visible on both preoperative whole bodyscan and regional scan. The means of WB SUVs, Reg SUVs and % SUV Changes of the 41 malignant nodes, 3.71±1.08, 5.18±1.60, and 42.59±33.41%, respectively, were all significantly higher than those of the 29 benign nodes, 2.45±0.73, 3.00±0.89, and 22.71±20.17%, respectively. ROC curve analysis gave sensitivity and specificity values of 80.5% and 82.8% at a cutoff of 2.89 (AUC 0.839) for WB SUVs, 87.8% and 82.8% at a cutoff of 3.61 (AUC 0.891) for Reg SUVs, and 87.8% and 41.4% at a cutoff of 12.3% (AUC 0.671) for % SUV Changes.**

Conclusion: **Additional, delayed regional FDG PET scans may improve the accuracy of lymph node staging of whole body FDG PET scan by providing additional criteria of Reg SUV and % SUV Change.** ***(Cancer Res Treat. 2005;37:114-121)***

Key Words: **Non-small cell lung cancer, Lymph node staging, FDG PET, Standardized uptake value**

INTRODUCTION

F-18 fluorodeoxyglucose (FDG) positron emission tomography (PET) is known to be an noninvasive method of staging the extracranial metastases of non-small cell lung cancer (NSCLC) patients (1). The primary reason for F-18 FDG PET referral in NSCLC patients is for lymph node staging (2). The accuracy of F-18 FDG PET in staging mediastinal lymph nodes of NSCLC patients is approximately 85%, compared to approximately 58% for chest computed tomography (CT) (1).

Correspondence: June-Key Chung, Department of Nuclear Medicine, Seoul National University College of Medicine, 28 Yeongeon-dong, Jongno-gu, Seoul 110-744, Korea. (Tel) 82-2-2072-3376, (Fax) 82-2-760-7690, (E-mail) jkchung@plaza.snu.ac.kr

Received February 24, 2005, Accepted March 21, 2005

*This study was supported by grant 0920020100 from the Clinical Research Institute of Seoul National University Hospital and in part by the Cancer Research Institute of Seoul National University College of Medicine.

The criteria currently used to differentiate malignant from benign lung lesions by F-18 FDG PET are based on either visual assessment or on a single time point, standardized uptake value (SUV). However, the differentiation of malignant from benign lesions is sometimes difficult, since considerable overlap occurs between the SUVs of these lesions.

In most PET centers, the SUVs of malignant lesions are calculated from F-18 FDG PET images with acquisition start 40～60 minutes after F-18 FDG injection (3,4). However, whereas the time taken to reach an SUV plateau in malignant lesions is known to be longer than 2 hours (5～8), that in most benign tumors and inflammatory lesions is known to be shorter, usually occurring within 2 hours (7,9～12). Therefore, the SUVs of F-18 FDG PET images of primary lesions that are delayed beyond the usual 40～60 minutes after F-18 FDG injection may be more accurate in the differentiation of malignant from benign lesions (7,9～11). However, no consensus has been reached on the usefulness of delayed F-18 FDG PET images for the differentiation of malignant from benign lesions in NSCLC patients.

In this study we undertook to determine whether additional, delayed regional FDG PET can increase the accuracy of lymph

node staging of F-18 whole body FDG PET in NSCLC patients by analyzing the SUVs of dissected lymph nodes that were visible by both F-18 whole body FDG PET and delayed regional FDG PET.

MATERIALS AND METHODS

1) Patients

Among the 87 consecutive patients who underwent open thoracotomy or mediastinoscopic biopsy of intrapulmonary, mediastinal or supraclavicular lymph nodes with suspicion of non-small cell lung cancer (NSCLC) within 1 month of F-18 FDG PET scan from September 2000 to August 2003, 35 patients had lymph nodes visible by both preoperative whole body scan and regional FDG PET scan and these 35 were included in this study. Patients who received anticancer chemotherapy or radiation therapy before the FDG PET scan were excluded. The male to female ratio was 29 : 6 and their mean age was 62.2±7.2 years (mean±S.D.; range 41～75 years). Thirty-two patients had NSCLC and the remaining 3 patients had infectious diseases of the lung. No patient had diabetes mellitus. Patient characteristics are summarized in Table 1.

Of the 290 lymph node stations dissected from the 87 patients, 70 lymph node stations from the above-mentioned 35 patients were visible by both preoperative whole body and regional FDG PET scan. Of these 70 visible lymph node stations, 29 were benign by histopathological examination and 41 were malignant. The locations of these 70 visible lymph node stations were 5 upper paratracheal nodes, 24 lower paratracheal nodes, 2 subaortic nodes, 14 subcarinal nodes, 23 N1 nodes and 2 supraclavicular nodes, according to the Naruke/ATS-LCSG (American Thoracic Society-North American Lung Cancer Study Group) map modified by Clifton F. Mountain and Carolyn M. Dresler (13).

Table 1. Patient characteristics

Characteristics	No. of patients (n=35)
Age (mean±s.d., yr)	62.2±7.2
M : F	29 : 6
Non-small cell lung cancer (n=32)	
Squamous cell carcinoma	14
Adenocarcinoma*	15
Large cell carcinoma	1
Poorly differentiated carcinoma	2
Benign infectious disease (n=3)	
Pulmonary tuberculosis	2
Pulmonary cryptococcosis	1

*Of 15 adenocarcinoma patients, 5 were mixed acinar and bronchioloalveolar cell carcinoma patients.

2) F-18 FDG PET scan

F-18 FDG PET scan was performed using an ECAT EXACT 47 PET scanner (CTI/Siemens, Knoxville, TN), which has 24 rings that provide 47 tomographic sections at 3.4 mm intervals. The system spatial resolution of the scanner was measured according to National Electrical Manufacturers Association NU2-2001 (14). The transaxial full-width at half-maximum (FWHM) measured at the center of the field of view was 6.7 mm, as was that measured at 10 cm from the center. The axial FWHM measured at the center of field of view was 7.8 mm and that measured at 10 cm from the center was 10.0 mm.

All patients fasted for at least 6 hours before the PET scan. Whole body 2 dimensional data acquisition was started, 65.2±20.4 minutes after injecting 370 MBq of F-18 FDG, in 5 bed positions (5-minute emission scan and 2-minute transmission scan per bed position). For each bed position, 5 planes were overlapped with contiguous bed positions. Additional, regional 2 dimensional data acquisition involving a 20-minute emission scan and an 8.5-minute transmission scan of the chest field was started 120.7±30.8 minutes after F-18 FDG injection. The mean interval between the start of whole body scan acquisition and the start of regional acquisition was 55.6±17.7 minutes. Triple Germanium-68 ring sources were used for the transmission scans. Transaxial images were reconstructed using a Gaussian filter (FWHM 6 mm) and corrected for attenuation using the attenuation map obtained from the transmission images. Both attenuation corrected whole body and regional images were reconstructed by ordered subsets expectation maximization method.

For each biopsy-proven visible lymph node station on whole body and regional PET scan, a small region of interest of 5～10 mm diameter was placed over the brightest area. SUV was calculated for each lymph node station as the decay-corrected ROI maximum count/tumor weight (kBq/g) divided by the injected activity/body weight (MBq/kg). Maximum SUV of whole body F-18 FDG PET (WB SUV), maximum SUV of the delayed chest regional F-18 FDG PET (Reg SUV), and the percent change in SUV between the WB and regional scans (% SUV Change) of each lymph node station were calculated.

$$\%\ \text{SUV Change} = \frac{\text{Reg SUV} - \text{WB SUV}}{\text{WB SUV}} \times 100\ (\%)$$

3) Diagnostic performance of F-18 Whole Body FDG PET on 290 dissected lymph node stations

Sensitivity, specificity, positive predictive value, negative predictive value and accuracy of F-18 Whole body FDG PET on visualizing the malignant lymph nodes of the 290 dissected lymph node stations were calculated.

4) Comparison of WB SUV, Reg SUV and % SUV Change between benign nodes and malignant nodes and analyses of receiver operating characteristic (ROC) curves

Means of the WB SUVs, Reg SUVs and % SUV Changes of the 41 malignant nodes were compared with those of the 29 benign nodes by using the Student's t-test. Analysis of ROC curves of WB SUVs, Reg SUVs and % SUV Changes were performed using MedCalc® Version 6.00. Sensitivities and specificities of WB SUVs, Reg SUVs and % SUV Changes at SUV cutoffs with the best diagnostic accuracy were calculated.

Areas under curve (AUCs) of WB SUVs, Reg SUVs and % SUV Changes were compared.

5) Comparison of the WB SUVs and Reg SUVs of the primary lung lesions of NSCLC patients

The WB SUVs, Reg SUVs and % SUV Changes of 82 malignant primary lung lesions and those of 8 benign lung lesions of the 87 consecutive patients were also calculated. The longest diameters of the primary lung lesions from gross pathology specimens or CT images ranged from 1.5～8.0 cm (3.7±1.6 cm, mean±S.D.).

6) Correlation analyses between WB SUVs and % SUV Changes of visible benign nodes, visible malignant nodes and malignant primary lung lesions

Correlation analyses were performed between WB SUVs and % SUV Changes for visible benign nodes, visible malignant nodes and malignant primary lung lesions. The correlation coefficient *r* and statistical significance were determined for each correlation analysis.

RESULTS

Sensitivity, specificity, positive predictive value, negative predictive value and accuracy of F-18 whole body FDG PET on visualizing malignant lymph nodes of the 290 dissected lymph node stations were 90.2%, 84.5%, 55.4%, 97.6% and 85.5%, respectively (Table 2).

Of the 70 dissected lymph nodes which were visible both on preoperative whole body and regional FDG PET scan, Reg SUVs of 40 out of the 41 malignant nodes were higher than their WB SUVs, while Reg SUV of one malignant node was lower that its WB SUV (WB SUV 4.88 to Reg SUV 4.72). Reg SUVs of 25 out of the 29 benign nodes were higher than their WB SUVs, while Reg SUVs of the remaining 4 benign nodes were lower than their WB SUVs (1.25 to 1.07, 2.54 to 2.30, 3.05 to 2.57 and 3.19 to 3.08) (Fig. 1～3).

The means of WB SUVs, Reg SUVs and % SUV Changes of the 41 malignant nodes, 3.71±1.08, 5.18±1.60, and 42.59 ±33.41%, respectively, were all significantly higher than those of the 29 benign nodes, 2.45±0.73, 3.00±0.89, and 22.71± 20.17%, respectively (Table 3).

ROC curve analysis gave sensitivity and specificity values of 80.5% and 82.8% at a cutoff of 2.89 (AUC 0.839) for WB SUVs, 87.8% and 82.8% at a cutoff of 3.61 (AUC 0.891) for Reg SUVs, and 87.8% and 41.4% at a cutoff of 12.3% (AUC

Table 2. Diagnostic performance of F-18 WB FDG PET on visualizing malignant lymph nodes of 290 dissected lymph node stations

		Visible lymph node on F-18 FDG PET	
		Positive	Negative
Histopathology	Positive	46	5
	Negative	37	202
Sensitivity	90.2%		
Specificity	84.5%		
Positive predictive value	55.4%		
Negative predictive value	97.6%		
Accuracy	85.5%		

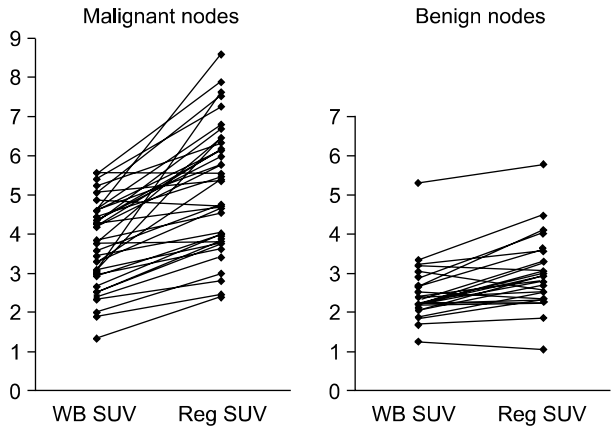

Fig. 1. Comparison of whole body maximum SUVs and regional maximum SUVs of 41 dissected malignant nodes and 29 dissected benign nodes which were visible on preoperative F-18 FDG PET.

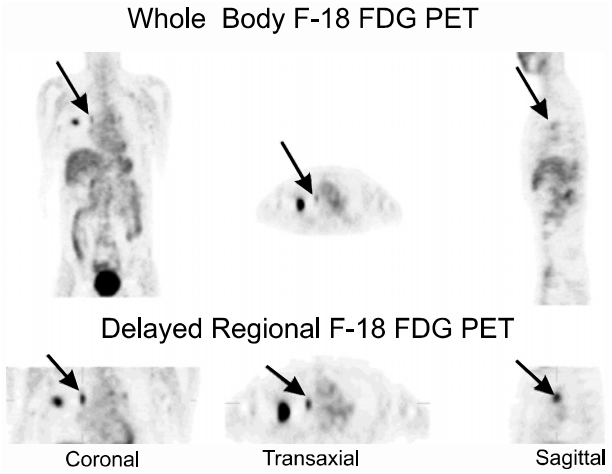

Fig. 2. Whole body F-18 FDG PET image (upper row) and delayed regional F-18 FDG PET image (lower row) of a 56-year-old man with adenocarcinoma in the upper lobe of the right lung. On the whole body PET image, only weak FDG accumulation was noted at 10R (right hilar) lymph node station; WB SUV was 1.33. On the regional PET image, however, FDG uptake was increased compared with the whole body PET image; Reg SUV was 2.39. Open thoracotomy biopsy revealed cancer cell invasion at this lymph node station.

0.671) for % SUV Changes (Fig. 4). The difference between AUCs of WB SUVs and Reg SUVs was 0.052 and this was not statistically significant (p=0.164). However, the difference between AUCs of WB SUVs and % SUV Changes was 0.168 (p=0.023), and the difference between AUCs of Reg SUVs and % SUV Changes was 0.220 ($p<0.001$), both of which were statistically significant.

Means of WB SUVs, Reg SUVs and % SUV Changes of the 82 malignant primary lung lesions were 8.31±4.06, 9.19±4.01 and 13.70±19.39, respectively, and those of the 8 benign lung lesions were 6.05±4.00, 6.38±3.42 and 13.24±17.15, respectively. The difference between the means of WB SUVs and Reg SUVs of the 82 malignant lesions was statistically significant ($p<0.01$, paired Student's t-test). However, of the 82 malignant lung lesions, 14 revealed decreased Reg SUVs compared with their WB SUVs.

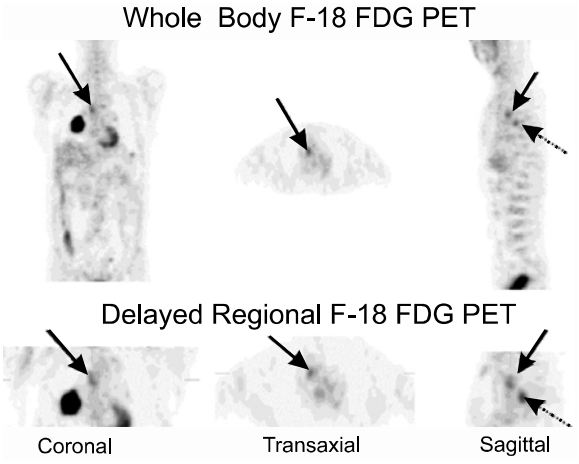

Fig. 3. Whole body F-18 FDG PET image (upper row) and delayed F-18 FDG PET image (lower row) of a 59-year-old man with squamous cell carcinoma in the middle lobe of the right lung. On the whole body PET image, FDG accumulation was noted at 4R (right lower paratracheal) lymph node station (arrows); WB SUV was 3.05. However, on the regional PET image, FDG uptake was decreased; Reg SUV was 2.57. Mediastinoscopic biopsy revealed no cancer cells in this lymph node. Dotted arrows show the 7 (subcarinal) lymph node station, which was invaded by cancer cells on mediastinoscopic biopsy. WB SUV was 3.08 and Reg SUV was 3.77.

The correlation between WB SUVs and % SUV Changes of the 29 visible benign nodes was not statistically significant (r=-0.10, p=0.59). The correlation between WB SUVs and % SUV Changes of the 41 visible malignant nodes tended toward negative correlation, but was not statistically significant (r=-0.30, p=0.057). However, a significant negative correlation was found between WB SUVs and % SUV Changes of the 82 malignant primary lung lesions (r=-0.38, p=0.0005) (Table 4, Fig. 5).

Of the 41 malignant lymph nodes that were visible both on preoperative whole body scan and regional scan, there were 16 nodes with WB SUV ≤3.0. The mean % SUV Change of these 16 malignant nodes with WB SUV ≤3.0 was 56.9±42.5 (range 21.1～145.9), while that of the other 25 malignant nodes with WB SUV ≤3.0 was 33.4±22.5 (range -3.3, -87.1). The difference was not statistically significant (p=0.056, Student's t-test). The % SUV Changes of 7 out of the 16 malignant nodes with WB SUV ≤3.0 were higher than 50%, and especially 5 showed % SUV Change ≥52%. However, all 29 benign lymph nodes that were visible both on preoperative whole body scan and regional scan showed % SUV Change <52% (Fig. 4C).

DISCUSSION

Lymph node staging is important for determining the operability of NSCLC patients, and the interpretation of mediastinal

Table 3. Comparison of mean values of WB SUV, Reg SUV, and % SUV change between benign nodes and malignant nodes which were visible on F-18 whole body FDG PET scan

	Benign nodes (n=29)	Malignant nodes (n=41)	Student's t-test* (p value)
WB SUV (mean±s.d.)	2.45±0.73	3.71±1.08	1.77×10^{-7}
Reg SUV (mean±s.d.)	3.00±0.89	5.18±1.60	5.52×10^{-10}
% SUV Change (mean±s.d.)	22.71±20.17	42.59±33.41	0.0029

*Unequal variances, two tails.

Table 4. Correlation analyses between WB SUVs and % SUV Changes of visible benign nodes, visible malignant nodes and malignant primary lung lesions

	Benign nodes (n=29)	Malignant nodes (n=41)	Malignant primary lung lesions (n=82)
Correlation coefficient	-0.10	-0.30	-0.38
95% C.I.* for correlation coefficient	-0.45 to 0.27	-0.56 to 0.0087	-0.55 to 0.17
p value	0.59	0.057	0.0005

*Confidence interval.

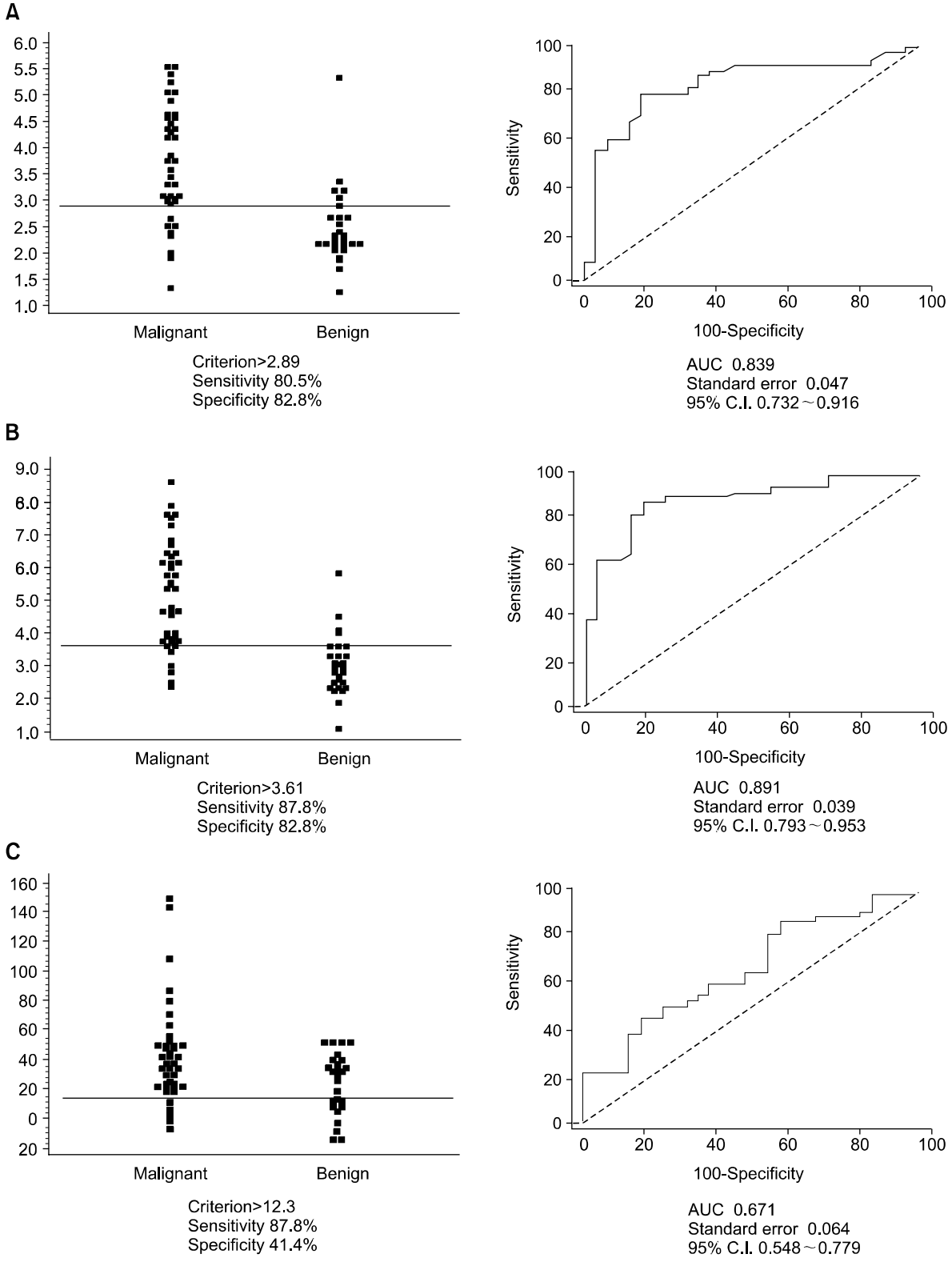

Fig. 4. (A) Plot of WB SUVs of 41 visible malignant nodes and 29 visible benign nodes (left) and ROC curve of WB SUVs (right). For a cut-off value of 2.89 WB SUV, the sensitivity was 80.5% and the specificity 82.8%. (B) Plot of Reg SUVs of the same nodes (left) and the ROC curve of Reg SUVs (right). For a cut-off value of 3.61 Reg SUV, the sensitivity was 87.8% and the specificity 82.8%. (C) Plot of percent change of SUVs (% SUV Changes) of the same nodes (left) and the ROC curve of % SUV Changes (right). For a cut-off value of 12.3 % SUV Change, the sensitivity was 87.8% and the specificity 41.4.

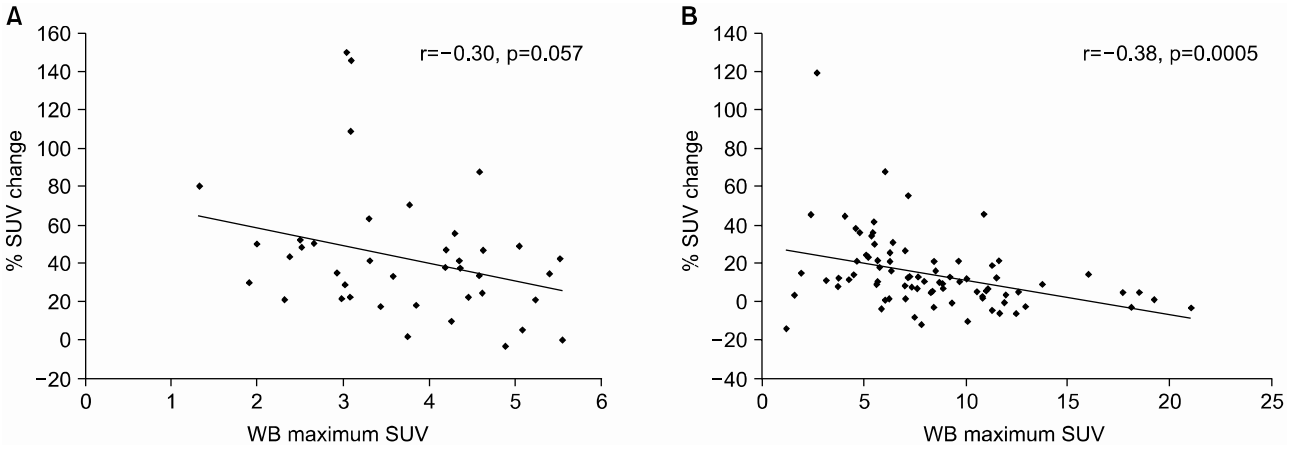

Fig. 5. (A) Correlation between WB SUVs and % SUV Changes of 41 dissected malignant nodes which were visible on FDG PET. Although there was a trend toward negative correlation, it did not reach statistical significance (r=-0.30, p=0.057). (B) Correlation between WB SUVs and % SUV Changes of 82 malignant primary lung lesions. A significant negative correlation was found (r=-0.38, p=0.0005).

lymph node stations as malignant or benign could change the treatment modality (1). F-18 FDG PET is known to be superior to CT at detecting extracranial metastases in NSCLC. However, most nuclear physicians rely on visual assessment or on a single time point SUV when interpreting lymph nodes on F-18 FDG PET images.

Currently, most PET centers use a whole body F-18 FDG PET protocol that starts data acquisition 40～60 minutes after F-18 FDG injection. This protocol was adopted on the basis of the findings of studies upon cerebral glucose metabolism (15,16). However, unlike brain tissue, FDG uptake in most malignant lesions does not plateau even 2 hours after FDG injection (5～8). Therefore, F-18 FDG PET images acquired within the 60 minutes following F-18 FDG injection may be inadequate for the differentiation of malignant and benign lesions.

By analyzing SUVs of visible lymph nodes on both whole FDG PET scan and regional scan of NSCLC patients, we found that Reg SUVs showed higher sensitivity and equal specificity in differentiating malignant nodes from benign nodes compared with WB SUVs, although the difference was not statistically significant. Furthermore, the % SUV Changes of malignant nodes were significantly higher than those of benign nodes.

Therefore, this study demonstrates, by using SUV analysis, the possibility of increasing the accuracy of lymph node staging in NSCLC patients by adding delayed regional F-18 FDG PET images to whole body F-18 FDG PET images. By performing additional, delayed regional FDG-PET imaging, one can also calculate Reg SUV and % SUV Change as well as WB SUV. Therefore, decisions on the operability of NSCLC patients can be based on a combination of three SUV criteria instead of only single time-point WB SUV.

In clinical practice, SUV has its role for the equivocal mediastinal lymph nodes of F-18 FDG PET images that might change the operability of NSCLC patients. In addition, it is not practical to perform delayed regional FDG PET scan for all NSCLC patients. In the present study, the negative predictive value for a non-visible lymph node on whole body FDG PET scan was 97.6%. Therefore, delayed regional FDG PET scan should be recommended only for NSCLC patients with visible equivocal mediastinal lymph nodes on whole body FDG PET scan that might change the treatment modality.

Although previous studies have reported that delayed FDG PET scans of primary lung cancer lesions showed increased SUVs compared with whole body FDG PET images performed earlier (11,17), 14 of the 82 pathologically-proven, primary lung cancer lesions showed decreased Reg SUVs compared with their WB SUVs in the present study. The mean % SUV Change of the 82 malignant lung lesions was only 13.70± 19.39%. This may partly be explained by the large size of primary lung lesions (mean 3.7±1.6 cm, range 1.5～8.0 cm by longest diameter) in the present study, which are expected to be more heterogeneous and to possess necrotic areas. Therefore, the maximum WB SUVs and Reg SUVs of some of these primary lung lesions could have been the maximum SUVs of necrotic areas (12). However, previous reports that applied maximum SUVs (8,10,17) or mean SUVs (7,9,11) for data analysis have shown increased SUVs in delayed FDG PET images, although no report mentioned lesion size. In the present study, the correlation between WB SUVS and the size (longest diameter) of the 82 primary lung lesions tended toward negative correlation, but was not statistically significant (r=-0.21, p=0.064). The reason for this divergent result needs to be studied further.

Some investigators have also reported that FDG uptake of benign lesions shows early peaks within 2 hours and that SUVs of delayed FDG PET images of benign lesions did not increase (7,9～12,18). However, according to our study result, 25 of the 29 benign nodes showed increased Reg SUVs. One important difference between our study protocol and that of former studies is that we used a longer acquisition time for the delayed regional FDG PET scans. To compensate for the low counts of the delayed regional FDG PET scan, we performed acquisition of the emission scan over 20 minutes, as compared

with 5-minute acquisition of emission scan per bed position for the whole body FDG PET scan. Perhaps a phantom study on WB SUV and Reg SUV might clear up this question.

Two former studies involving delayed FDG PET scan of malignant lymph nodes reported opposite results. Boerner et al. (8) reported that in breast cancer patients, 3-hour delayed, whole body FDG PET scanning detected more metastatic lymph nodes than 1.5-hour, whole body FDG PET imaging. In contrast, Kubota et al. (17) reported that the SUVs of mediastinal lymph nodes by 2-hour delayed, whole body FDG PET scanning were no higher than those by 1-hour, whole body FDG PET scanning. The emission scan time per bed position was not mentioned in the former study, and was 3 minutes for a 1-hour image and 4 minutes for a 2-hour image in the latter study. Therefore, it is unclear whether acquisition time differences are responsible for different study results. However, in the present study, one malignant lymph node showed lower Reg SUV than its WB SUV, while other malignant nodes of the same patient showed higher Reg SUVs (Fig. 3). Therefore, although differences in acquisition time of whole body scan and regional scan might have some effect on the higher mean value of Reg SUVs of malignant nodes, the individual difference of % SUV Change can not be explained only by the acquisition time. The recent study of Demura et al has demonstrated the higher diagnostic performance of 3-hour delayed PET scan compared to 1-hour PET scan in the lymph node staging of thoracic malignancies (19).

The advantage of delayed PET scanning lies in the increased target-to-background ratio, especially in malignant lesions. However, decreased counts could limit the detection of small lesions. As the primary objective of whole body FDG PET scan is lesion detection, it is desirable to perform whole body FDG PET scan early, at around 60 minutes after FDG injection, when the count statistics are favorable. Furthermore, to differentiate known lesions as malignant or benign, it is desirable to perform another FDG PET scan later at 2 or 3 hours after FDG injection (7).

CONCLUSIONS

Reg SUVs showed higher sensitivity and equal specificity in differentiating malignant nodes from benign nodes of NSCLC patients, when compared with WB SUVs, although the difference was not statistically significant. Percent SUV Changes of malignant nodes were significantly higher than those of benign nodes.

Additional, delayed regional FDG PET scans may improve the accuracy of lymph node staging of whole body FDG PET scan by providing additional criteria of Reg SUV and % SUV Change.

ACKNOWLEGMENTS

The authors thank Hong Jae Lee for his excellent technical assistance.

REFERENCES

1. Hagge RJ, Wong TZ, Coleman RE. Positron emission tomography: brain tumors and lung cancer. Radiol Clin North Am. 2001;39:871-81.
2. Seltzer MA, Yap CS, Silverman DH, Meta J, Schiepers C, Phelps ME, et al. The impact of PET on management of lung cancer: the referring physician's perspective. J Nucl Med. 2002;43:752-6.
3. Hoh CK, Hawkins RA, Glaspy JA, Dahlbom M, Tse NY, Hoffman EJ, et al. Cancer detection with whole-body PET using 2-[^{18}F]Fluoro-2-deoxy-D-glucose. J Comput Assist Tomogr. 1993;17:582-9.
4. Lowe VJ, DeLong DM, Hoffman JM, Coleman RE. Optimum scanning protocol for FDG-PET evaluation of pulmonary malignancy. J Nucl Med. 1995;36:883-7.
5. Fischman AJ, Alpert NM. FDG-PET in oncology: there's more to it than looking at pictures. J Nucl Med. 1993;34:6-11.
6. Hamberg LM, Hunter GJ, Alpert NM, Choi NC, Babich JW, Fischman AJ. The dose uptake ratio as an index of glucose metabolism: useful parameter or oversimplification? J Nucl Med. 1994;35:1308-12.
7. Lodge MA, Lucas JD, Marsden PK, Cronin BF, ODoherty MJ, Smith MA. A PET study of ^{18}FDG uptake in soft tissue masses. Eur J Nucl Med. 1999;26:22-30.
8. Boerner AR, Weckesser M, Herzog H, Schmitz T, Audretsch W, Nitz U, et al. Optimal scan time for fluorine-18 fluorodeoxyglucose positron emission tomography in breast cancer. Eur J Nucl Med. 1999;26:226-30.
9. Hustinx R, Smith RJ, Benard F, Rosenthal DI, Machtay M, Farber LA, et al. Dual time point fluorine-18 fluorodeoxyglucose positron emission tomography: a potential method to differentiate malignancy from inflammation and normal tissue in the head and neck. Eur J Nucl Med. 1999;26:1345-8.
10. Zhuang H, Pourdehnad M, Lambright ES, Yamamoto AJ, Lanuti M, Li P, et al. Dual time point ^{18}F-FDG PET imaging for differentiating malignant from inflammatory processes. J Nucl Med. 2001;42:1412-7.
11. Matthies A, Hickeson M, Cuchiara A, Alavi A. Dual time point 18F-FDG PET for the evaluation of pulmonary nodules. J Nucl Med. 2002;43:871-5.
12. Kubota R, Kubota K, Yamada S, Tada M, Ido T, Tamahashi N. Microautoradiographic study for the differentiation of intratumoral macrophages, granulation tissues and cancer cells by the dynamics of fluorine-18-fluorodeoxyglucose uptake. J Nucl Med. 1994;35:104-12.
13. Mountain CF, Dresler CM. Regional lymph node classification for lung cancer staging. Chest. 1997;111:1718-23.
14. National Electrical manufacturers Association. NEMA Standards Publication *NU2-1994*. Washington DC: National Electrical Manufacturers Association. 1994.
15. Reivich M, Alavi A, Wolf A, Fowler J, Russell J, Arnett C, et al. Glucose metabolic rate kinetic model parameter determination in humans: the lumped constants and rate constants for [^{18}F]fluorodeoxyglucose and [^{11}C]deoxyglucose. J Cereb Blood Flow Metab. 1985:5:179-92.

16. Nolop KB, Rhodes CG, Brudin LH, Beaney RP, Krausz T, Jones T, et al. Glucose utilization in vivo by human pulmonary neoplasms. Cancer. 1987;60:2682-9.
17. Kubota K, Itoh M, Ozaki K, Ono S, Tashiro M, Yamaguchi K, et al. Advantage of delayed whole-body FDG-PET imaging for tumour detection. Eur J Nucl Med. 2001;28:696-703.
18. Yamada S, Kubota K, Kubota R, Ido T, Tamahashi N. High accumulation of fluorine-18-fluorodeoxyglucose in turpentine-induced inflammatory tissue. J Nucl Med. 1995;36:1301-6.
19. Demura Y, Tsuchida T, Ishizaki T, Mizuno S, Totani Y, Ameshima S, et al. ^{18}F-FDG accumulation with PET for differentiation between benign and malignant lesions in the thorax. J Nucl Med. 2003;44:540-8.